


# RGB mass loss: inferences from CMD-fitting and asteroseismology

Marco Tailo 

Dipartimento di Fisica e Astronomia Augusto Righi, Università degli Studi di Bologna,  
Via Gobetti 93/2, I-40129 Bologna, Italy  
email: [mrctailo@gmail.com](mailto:mrctailo@gmail.com), [marco.tailo@unibo.it](mailto:marco.tailo@unibo.it)

**Abstract.** The amount of mass lost by stars during the red-giant branch (RGB) phase is one of the main parameters needed to fully understand later stages of stellar evolution. In spite of its importance, a fully-comprehensive physical understanding of this phenomenon is still missing, and we, mostly, rely on empirical formulations. The Galactic Globular Clusters are ideal targets to derive such formulations, but, until recently, the presence of multiple populations has been a major challenge.

We will discuss the insights on RGB mass loss that can be obtained from the study of the horizontal branch stars in such stellar associations. The estimates obtained via the study of the photometric data will be compared with recent and newly obtained estimates derived for few high metallicity open clusters and a large sample of field stars with asteroseismic techniques.

**Keywords.** stars: Hertzsprung-Russell diagram; stars: horizontal-branch; stars: mass loss; stars: fundamental parameters

---

## 1. Introduction

Determining the mass loss along the Red Giant Branch (RGB) is a crucial step to fully understand later stages of stellar evolution and by some extent understand the fate of planetary systems. The comparison between the stellar mass of the helium-burning- and the RGB-stars provides an efficient approach to infer the RGB mass loss in simple stellar populations.

In the old globular clusters (GCs) the helium burning stars are hosted on the Horizontal Branch (HB). These stars reach their position along the branch, at higher effective temperatures than their progenitors, after the degenerate helium in their core has ignited during the Helium flash at the Tip of the RGB. The total mass deficit, if any, of the resulting stars with respect to the RGB ones represents the sought-after mass loss. Recent works (Tailo et al. 2020, 2021; T20, T21) have introduced an innovative approach, based on the comparison of the photometric data with state of the art stellar population models, to infer the mass loss of the distinct stellar populations in GCs and applied this method to a large sample of more than 50 old, low metallicity GCs; also including those GCs without evidence of multiple stellar populations.

In younger and in metal rich ( $[\text{Fe}/\text{H}] > -0.3$ ) clusters the helium burning stars are clustered in a smaller portion of the colour magnitude diagram; this new locus is dubbed Red Clump (RC) to distinguish it from the HB (see Girardi 2016 for a general review). The relatively large interval of mass values of the RC stars, compared to the small colour extension of this locus, makes difficult to get accurate mass and mass loss estimates with photometric tools alone. Therefore, an approach involving asteroseismic techniques is more appropriate and can lead to better mass estimates.

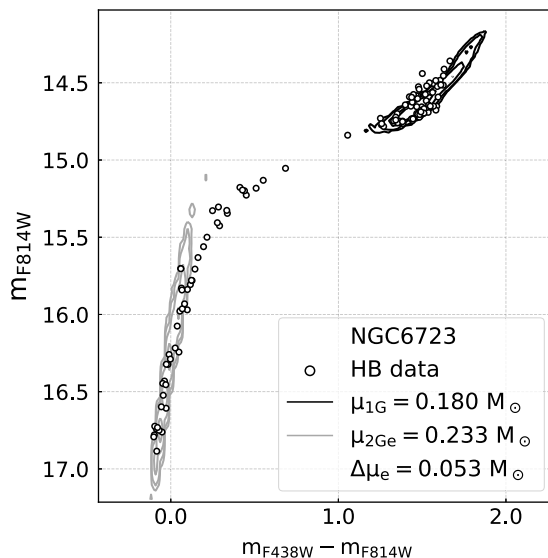


**Figure 1.** An example of the simulation realized in our study to obtain an estimate of the mass loss in the stellar population in the Galactic GCs. The photometric data of NGC 6723 are represented as white points. The black and the grey contour plots represent the best fit simulations for the 1G and the 2Ge stars in this cluster. An additional mass loss ( $\Delta\mu$ ) is required to correctly describe the latter population.

The comparison of the results coming from the old, metal poor GCs and the asteroseismic study of the mass loss in the young metal rich clusters can give new insight on the complexity of the mass loss in RGB stars.

## 2. Mass loss in old GCs

The large majority of the old Galactic GCs host two kinds of stellar populations: a first generation (1G) of stars, characterized by abundance patterns similar to the field stars of comparable metallicity, and a second generation (2G), showing different patterns and enhanced helium abundance (see Milone et al. 2017, 2018 and Marino et al. 2019 for a review of the observational framework). The mechanism and the evolutionary path leading to the formation of these multiple populations are still largely debated (see Renzini et al. 2015 and Bastian & Lardo 2018 for a review of the theoretical framework) and no conclusive theoretical explanation and unified evolutionary scenario has been developed.

On the HB these two kinds of population can easily be distinguished. On the basis of the spectroscopic results (from e.g. Marino et al. 2008) and seminal theoretical works (D'Antona et al. 2002), in most GCs it is possible to identify the 1G stars with the reddest group of stars along the HB, and the 2G with the others. Among the various groups forming the 2G, the extreme part (2Ge), corresponding to the most enhanced sub-stellar populations occupies the bluest end of the HB.

The parameter degeneracy, traditionally associated to the effects of mass loss and helium, can be broken for both groups of stars adopting either the primordial helium abundance, for the 1G, or the helium values provided by e.g. Milone et al. (2018), in the case of the 2Ge. Therefore the last parameter to be evaluated is the integrated mass loss of the two stellar populations.

By comparing the photometric data with stellar populations models such mass loss estimates can be achieved. An example is shown in Fig. 1 for the cluster NGC 6723. The

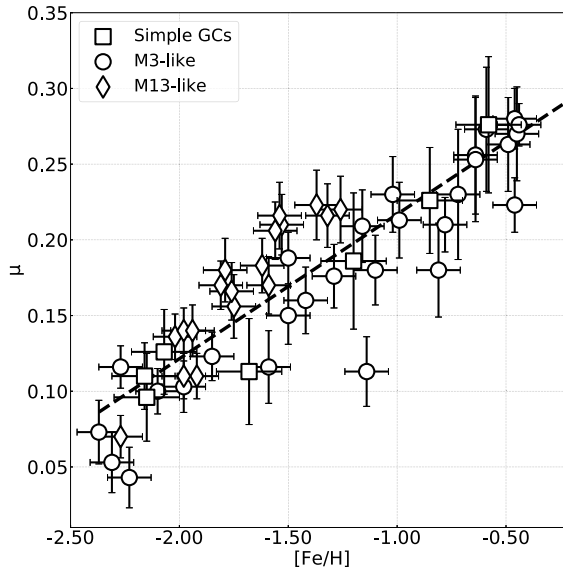


**Figure 2.** *Left panel:* Integrated mass loss of the first generation stars in the GC sample analysed in our works (T20,T21). The three series of points represent simple population clusters, M3-like and M13-like GCs, respectively as squares, circles and diamonds.

best fit simulations for the 1G and the 2Ge are selected with the T20 and T21 method, to whom we refer for further details, and are represented with black and grey contour plots in the figure. For the 1G stars we found a mean mass of  $M_{\text{RGB}}^1 = 0.827 \pm 0.014 M_{\odot}$  and  $M_{\text{HB}}^1 = 0.647 \pm 0.023 M_{\odot}$ , respectively for the RGB and HB stars, whereas for the 2Ge stars we found  $M_{\text{RGB}}^{2\text{Ge}} = 0.793 \pm 0.016 M_{\odot}$  and  $M_{\text{HB}}^{2\text{Ge}} = 0.560 \pm 0.024 M_{\odot}$ . These values give integrated RGB mass loss values of  $\mu_{1\text{G}} = 0.180 \pm 0.023 M_{\odot}$  and  $\mu_{2\text{Ge}} = 0.233 \pm 0.024 M_{\odot}$  respectively, for the 1G and 2Ge stars.

If we look at the results for all the clusters analysed in our works we see that a relation between the integrated mass loss and the parameters of the host clusters emerge. While we refer to T20 and T21 for the full discussion, we examine here what we deem to be the most important one, as it is connected to the evolution of the early cluster. Indeed, if we look at the mass loss of the 1G stars as a function of cluster metallicity, left panel of Figure 2, we see that a strong relation is present. In the figure we represent the least square best fit line that can be derive from the data as the dashed black line. The relation can also be described via the following equation:  $\mu = (0.095 \pm 0.006) \times [\text{Fe}/\text{H}] + (0.312 \pm 0.011)$ . If we convert these value in mass loss rate via the most commonly used Reimers (1975) formula ( $\eta_{\text{R}}$ ), we get that the free parameter in the model has to vary from a minimum of  $\eta_{\text{R}} \sim 0.05$  at  $[\text{Fe}/\text{H}] \sim -2.4$  to a maximum of  $\eta_{\text{R}} \sim 0.60$  at  $[\text{Fe}/\text{H}] \sim -0.5$  (T20).

In Figure 3 we compare the integrated mass loss obtained with our relation with the others present in the literature. For the old Galactic GCs, we reported the results from Gratton et al. (2010), black and Origlia et al. 2014). We report the results from Savino et al. (2019) for the Tucana dSph galaxy and from Salaris et al. (2013) for the Sculptor dSph galaxy. Finally more example of similar trends, albeit for a smaller sample of GCs, can be found in VandenBerg et al. (2016); Denissenkov et al. (2017); VandenBerg & Denissenkov (2018). Furthermore the mass loss rate we obtain here can also be compared with the ones in McDonald & Zijlstra (2015, and references therein), where the authors, using the results from Gratton et al. (2010), found an almost constant  $\eta_{\text{R}} = 0.477 \pm 0.070$  for the entire range of metallicities.

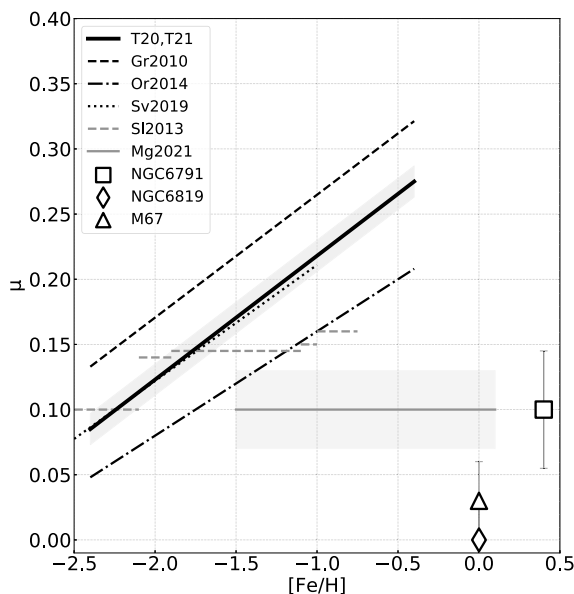


**Figure 3.** Comparison of the mass loss law obtained from our results (solid black) and few other relations and estimate found in the literature. T20,T21: [Miglio et al. 2021](#); [Tailo et al. 2021](#); Gr2010: [Gratton et al. 2010](#); Or2014: [Origlia et al. 2014](#); Sv2019: [Savino et al. 2019](#); Sl2013: [Salaris et al. 2013](#); Mg2021: [Miglio et al. 2021](#); NGC6791 from [Miglio et al. 2012](#) and NGC6819 from [Miglio et al. 2012](#) and [Handberg et al. 2017](#). M67 from [Stello et al. \(2016\)](#) See text for details.

The fact that most of these relations, obtained for the old stellar populations and with different methods, share the same slope, suggests that RGB evolution could be universal in old stellar associations like GCs and dSph.

### 3. Extending to higher metallicity range

The analysis of the helium burning stars, and, consequently, the estimate of the mass loss, in higher metallicity or younger GCs is trickier. When the metallicity is high enough, or the age low enough, the HB collapse in a small region of the CMD and is dubbed Red Clump (RC), to distinguish it from the HB.

The tracks hosted in this region are clumped together in a small area but cover a relatively large interval of mass values (see e.g. [Girardi 2016](#)) compared to their HB counterparts. This makes obtaining accurate mass estimate difficult with photometric tools only, and a combination of tools from different fields is necessary to reach good precision.

Among the tools available, asteroseismology is able to provide precise estimates of the mass of these stars while at the same time it allows to avoid most of the difficulties encountered with photometric techniques. We refer to [Chaplin & Miglio \(2013\)](#) and [Aerts \(2021\)](#) for a general overview. In a nutshell, continuous photometric observations of cool stars (giants, in particular) can be used to detect solar-like oscillations and spectra. Constraints from these spectra can be combined with surface properties to infer precise stellar masses. If we apply then these techniques to both helium burning and RGB stars we also get a more precise estimate of mass loss. This has been indeed performed on few young, high metallicity Galactic open clusters.

In an early work, [Miglio et al. \(2012\)](#) performed the asteroseismological analysis of the two young, high metallicity clusters NGC6791 and NGC6819. For NGC6791 Miglio and

collaborators estimated the integrated mass loss to be  $\sim 0.10 \pm 0.02 M_{\odot}$ . For NGC6819 by Miglio and collaborators a mean mass of  $1.61 \pm 0.02 M_{\odot}$  and  $1.62 \pm 0.03 M_{\odot}$ , respectively for the RGB and RC stars. Therefore they estimate an almost absent mass loss. Recently the mass and mass loss estimates for NGC6819 have been updated by Handberg et al. (2017) confirming the results by Miglio and collaborators.

Another example of the evaluation of mass loss done via asteroseismic techniques can be found for the open cluster M67 (Stello et al. 2016). Stello and collaborators analysed a large number of RGB stars and a conspicuous sample of RC stars finding no evidence of strong mass loss.

An extensive analysis of the mass and the mass loss of a large number of stars can be found in Miglio et al. (2021). In this paper the authors analyse a large number of field stars in the Kepler field. When combining the mass and age information with the  $[\text{Fe}/\text{H}]$  and  $[\alpha/\text{Fe}]$  values coming from the APOGEE DR14 (Abolfathi et al. 2018), their main results an average  $0.1 M_{\odot}$  of mass loss for the old (older than 4Gyr), high  $[\alpha/\text{Fe}]$  stars ( $[\alpha/\text{Fe}] > 0.1$ ) in the sample.

We included the results from Miglio et al. 2021 for the stars in the Kepler field in the right panel of Figure 3 as the grey solid line; the shaded area approximately represent the  $1\sigma$  interval. In similar way the results for NGC 6791 from Miglio et al. 2012 and for NGC6819 from Miglio et al. 2012 and Handberg et al. 2017 are also reported. Finally we included the results from Stello et al. (2016).

#### 4. A missing piece of the puzzle?

The comparison between the results coming from the high metallicity stars with the ones obtained for the old, low metallicity stellar populations in GCs or dSph galaxies shows a discrepancy.

Indeed, it seems to be tension between the mass loss predicted by the empirical relations described in Figure 3 at solar and higher metallicity values and the direct observations carried out with asteroseismic techniques. This may be the result of our incomplete understanding of the phenomenon of mass loss or of still unknown interaction with the formation environment. Finally, as younger, more massive stars have lower RGB Tip luminosities (for fixed metallicity and helium values, see e.g. Serenelli et al. 2017) it is also possible that the low, integrated mass loss is consequence of the higher surface gravity of these stars.

This would make the relations presented in Figure 3 valid only in those range of metallicity or age values or even valid only for these specific class of stellar associations. However investigating the origin of such discrepancy is beyond the scope of this work as it would need accurate simulation and observation of early clusters.

#### References

- Abolfathi B., Aguado D. S., Aguilar G., Allende Prieto C., Almeida A., Ananna T. T., Anders F., et al., 2018, *ApJS*, 235, 42. doi:10.3847/1538-4365/aa9e8a
- Aerts C., 2021, *RvMP*, 93, 015001. doi:10.1103/RevModPhys.93.015001
- Bastian N., Lardo C., 2018, *ARA&A*, 56, 83. doi:10.1146/annurev-astro-081817-051839
- Chaplin W. J., Miglio A., 2013, *ARA&A*, 51, 353. doi:10.1146/annurev-astro-082812-140938
- D'Antona F., Caloi V., Montalbán J., Ventura P., Gratton R., 2002, *A&A*, 395, 69. doi:10.1051/0004-6361:20021220
- Denissenkov P. A., VandenBerg D. A., Kopacki G., Ferguson J. W., 2017, *ApJ*, 849, 159. doi:10.3847/1538-4357/aa92c9
- Girardi L., 2016, *ARA&A*, 54, 95. doi:10.1146/annurev-astro-081915-023354
- Gratton R. G., Carretta E., Bragaglia A., Lucatello S., D'Orazi V., 2010, *A&A*, 517, A81. doi:10.1051/0004-6361/200912572

- Handberg R., Brogaard K., Miglio A., Bossini D., Elsworth Y., Slumstrup D., Davies G. R., et al., 2017, *MNRAS*, 472, 979. doi:10.1093/mnras/stx1929
- Marino A. F., Villanova S., Piotto G., Milone A. P., Momany Y., Bedin L. R., Medling A. M., 2008, *A&A*, 490, 625. doi:10.1051/0004-6361:200810389
- Marino A. F., Villanova S., Milone A. P., Piotto G., Lind K., Geisler D., Stetson P. B., 2011, *ApJL*, 730, L16. doi:10.1088/2041-8205/730/2/L16
- Marino A. F., Milone A. P., Renzini A., D'Antona F., Anderson J., Bedin L. R., Bellini A., et al., 2019, *MNRAS*, 487, 3815. doi:10.1093/mnras/stz1415
- McDonald I., Zijlstra A. A., 2015, *MNRAS*, 448, 502. doi:10.1093/mnras/stv007
- Miglio A., Brogaard K., Stello D., Chaplin W. J., D'Antona F., Montalbán J., Basu S., et al., 2012, *MNRAS*, 419, 2077. doi:10.1111/j.1365-2966.2011.19859.x
- Miglio A., Chiappini C., Mackereth J. T., Davies G. R., Brogaard K., Casagrande L., Chaplin W. J., et al., 2021, *A&A*, 645, A85. doi:10.1051/0004-6361/202038307
- Milone A. P., Piotto G., Renzini A., Marino A. F., Bedin L. R., Vesperini E., D'Antona F., et al., 2017, *MNRAS*, 464, 3636. doi:10.1093/mnras/stw2531
- Milone A. P., Marino A. F., Renzini A., D'Antona F., Anderson J., Barbuy B., Bedin L. R., et al., 2018, *MNRAS*, 481, 5098. doi:10.1093/mnras/sty2573
- Origlia L., Ferraro F. R., Fabbri S., Fusi Pecci F., Dalessandro E., Rich R. M., Valenti E., 2014, *A&A*, 564, A136. doi:10.1051/0004-6361/201423617
- Reimers D., 1975, *MSRSL*, 8, 369
- Renzini A., D'Antona F., Cassisi S., King I. R., Milone A. P., Ventura P., Anderson J., et al., 2015, *MNRAS*, 454, 4197. doi:10.1093/mnras/stv2268
- Salaris M., de Boer T., Tolstoy E., Fiorentino G., Cassisi S., 2013, *A&A*, 559, A57. doi:10.1051/0004-6361/201322501
- Savino A., Tolstoy E., Salaris M., Monelli M., de Boer T. J. L., 2019, *A&A*, 630, A116. doi:10.1051/0004-6361/201936077
- Serenelli A., Weiss A., Cassisi S., Salaris M., Pietrinferni A., 2017, *A&A*, 606, A33. doi:10.1051/0004-6361/201731004
- Stello D., Vanderburg A., Casagrande L., Gilliland R., Silva Aguirre V., Sandquist E., Leiner E., et al., 2016, *ApJ*, 832, 133. doi:10.3847/0004-637X/832/2/133
- Tailo M., Milone A. P., Lagioia E. P., D'Antona F., Jang S., Vesperini E., Marino A. F., et al., 2021, *MNRAS*, 503, 694. doi:10.1093/mnras/stab568
- Tailo M., Milone A. P., Lagioia E. P., D'Antona F., Marino A. F., Vesperini E., Caloi V., et al., 2020, *MNRAS*, 498, 5745. doi:10.1093/mnras/staa2639
- VandenBerg D. A., Denissenkov P. A., 2018, *ApJ*, 862, 72. doi:10.3847/1538-4357/aaca9b
- VandenBerg D. A., Denissenkov P. A., Catelan M., 2016, *ApJ*, 827, 2. doi:10.3847/0004-637X/827/1/2